

# Realization of an analog predistortion circuit for RF optical fiber links\*

Tian Xuenong(田学农), Wang Zhigong(王志功)<sup>†</sup>, and Li Wei(李伟)

(Institute of RF- & OE-ICs, Southeast University, Nanjing 210096, China)

**Abstract:** This paper presents an analog predistortion circuit for RF optical fiber links. The circuit consists of two source-coupled differential transconductance amplifiers which could provide linear and nonlinear transfer characteristics by adjusting the bias voltage and the transistor sizes. The circuit was designed and realized in a standard 0.18- $\mu\text{m}$  CMOS technology of SMIC. The chip occupies  $0.48 \times 0.24 \text{ mm}^2$ . The DC supply is 3.3 V. Using this circuit, the third-order intermodulation distortion (IMD) suppression of a directly modulated RF optical fiber link can be improved by 9–16 dBc at relatively low cost.

**Key words:** analog predistortion; intermodulation distortion; optical fiber links

**DOI:** 10.1088/1674-4926/30/11/115005

**EEACC:** 2570

## 1. Introduction

An ROF (radio over fiber) link means that the information is transported over an optical fiber by modulating the light with a radio signal either at carrier frequency or at intermediate frequency. Such a link has the advantages of low signal attenuation, large bandwidth, light weight, and immunity to electromagnetic interference. Therefore, it is an attractive alternative compared to other transporting media and has been used in a variety of applications including antenna remoting<sup>[1]</sup>, cable television distribution systems, microcellular networks, and optically controlled phased array radars<sup>[2,3]</sup>. One primary limitation on the performance of ROF links is the nonlinearity which is caused by fiber link components, particularly laser diodes<sup>[4]</sup>. The dynamic range and the bandwidth efficiency of the ROF link are severely degraded by the nonlinearity distortion of the link.

To reduce the nonlinear distortion of the ROF link, various linearization schemes have been proposed and implemented. These techniques can be broadly categorized into linearization in the optical domain and linearization in the electrical domain. Both of these techniques offer comparable performance in the linearization of the ROF link, but electronic linearization has significant economic advantages. Many optical linearization techniques involve the use of additional optical components and the cost is increased significantly<sup>[5,6]</sup>. Electronic analog predistortion is one of the techniques to reduce nonlinear distortion in the electrical domain; it is relatively simple to implement and its cost is relatively low. The signal is predistorted and the intermodulation product is purposely generated to cancel the intermodulation distortion caused by the ROF link. Lin<sup>[7]</sup> proposed and implemented an analog predistortion circuit for RF optical links in AMS 0.35- $\mu\text{m}$  CMOS, but so far there have been no further reports on this circuit. In this paper, our design and the measurement results for the

circuit will be reported.

## 2. Circuit principle

A mathematical model of the predistortion system is illustrated in Fig. 1. For convenience a simplified nonlinear model of the ROF link is used and only second- and third-order nonlinearities of the system are considered. The predistortion block is placed before the RF optical fiber link and it introduces distortion in the input signal. Then the predistorted signal combines with the distortion generated by the RF optical fiber link and the overall distortion should cancel out.

The input-output relationship of the predistortion system shown in Fig. 1 can be expressed as

$$Y_{\text{out}} = \alpha X_{\text{in}} + (ab + \beta a^2) X_{\text{in}}^2 + (\alpha c + 2\beta ab + \gamma a^3) X_{\text{in}}^3 + \dots \quad (1)$$

The second- and third-order distortions can be cancelled by adjusting the coefficients of the predistortion block to meet the following relationship:

$$ab + \beta a^2 = 0, \quad (2)$$

$$\alpha c + 2\beta ab + \gamma a^3 = 0. \quad (3)$$

An analog predistorter which could generate a polynomial relationship with adjustable coefficients is realized in this paper. The basic cell of the predistorter is a source coupled differential amplifier as shown in Fig. 2.

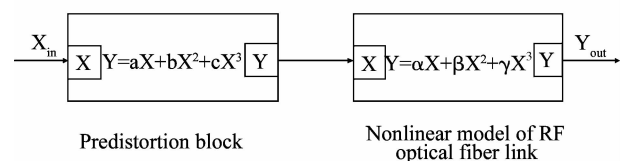


Fig. 1. Predistortion system block diagram.

\* Project supported by the High-Tech-Program of China (No. 2007AA01Z2a5).

<sup>†</sup> Corresponding author. Email: zgwang@seu.edu.cn

Received 26 March 2009, revised manuscript received 26 June 2009

© 2009 Chinese Institute of Electronics

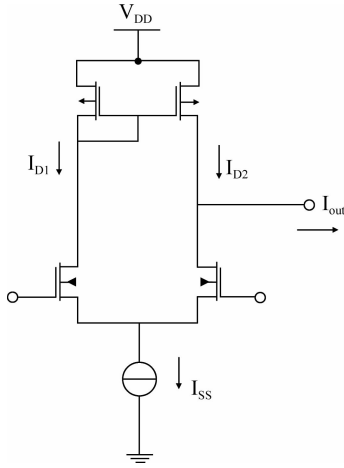


Fig. 2. Circuit diagram of the source coupled differential amplifier.

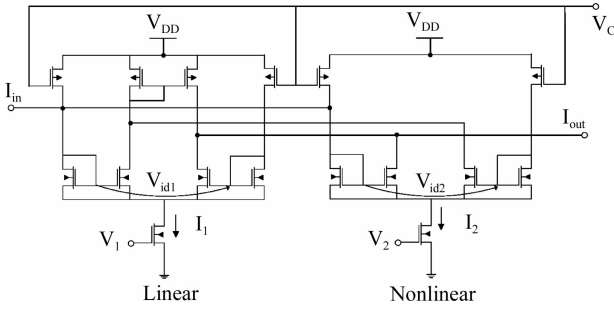


Fig. 3. Circuit diagram of the analog predistortion circuit.

For such an amplifier, the differential output current and input voltage are related by

$$I_o = I_{D1} - I_{D2} = \sqrt{K}V_{id} \sqrt{2I_{ss} - KV_{id}^2} = \sqrt{2KI_{ss}} \left( V_{id} - \frac{1}{2} \frac{V_{id}^3}{2I_{ss}/K} - \frac{1}{2} \frac{1}{4} \frac{V_{id}^5}{(2I_{ss}/K)^2} \dots \right), \quad (4)$$

where  $K = (1/2)\mu_n C_{ox} W/L$ ,  $\mu_n$  is the effective carrier mobility of the MOS device,  $C_{ox}$  is the gate oxide capacitance per unit area,  $W$  is the channel width,  $L$  is the channel length, and  $V_{id}$  is the differential input voltage. The output current can be expressed as a power series of  $V_{id}$ . By adjusting the value of  $I_{ss}$  or  $W/L$  of the device, different transfer characteristics could be obtained.

As shown in Fig. 3, the analog predistortion circuit is composed of two source coupled differential transconductance amplifiers. The circuit has three control voltages to adjust the transfer characteristics.  $V_1$  and  $V_2$  are the bias voltages for the source current sink of the linear and nonlinear differential transconductance amplifiers respectively.  $V_C$  is the control voltage for the PMOS transistors which are used as the active load of the differential amplifiers. All the transistors should be operated in the saturation region.

By adjusting the size and the bias of each transconductance amplifier, the linear and nonlinear transfer characteristics could be obtained. In the linear part, the bias voltage  $V_1$  and the  $W/L$  of the transistors of the differential amplifier are chosen to let the  $I_{ss}/K$  of Eq. (4) be large enough, so that

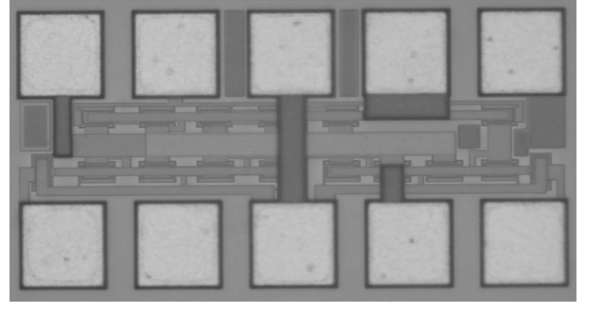


Fig. 4. Photograph of the analog predistortion circuit chip.

the output current is approximately proportional to the input differential voltage and is given by

$$I_{OUT(LIN)} = \sqrt{2KI_1} V_{id1} = G_{lin} V_{id1}, \quad (5)$$

where  $V_{id1}$  is the differential input voltage applied to the linear differential transconductance amplifier.

In the nonlinear part of the predistortion circuit, an appropriate choice of the bias voltage  $V_2$  and the  $W/L$  of the transistors should be made so that the nonlinear terms cannot be omitted and the output current is given by

$$I_{OUT(NONLIN)} = \sqrt{2KI_2} \left[ V_{id2} - \frac{V_{id2}^3}{4I_2/K} - \frac{V_{id2}^5}{32(I_2/K)^2} + \dots \right] = G_{nonlin} \left[ V_{id2} - \frac{V_{id2}^3}{4I_2/K} - \frac{V_{id2}^5}{32(I_2/K)^2} + \dots \right]. \quad (6)$$

The total output current could be given as

$$I_{OUT} = I_{OUT(LIN)} - I_{OUT(NONLIN)} = (G_{lin} V_{id1} - G_{nonlin} V_{id2}) + G_{nonlin} \left( \frac{V_{id2}^3}{4I_2/K} + \frac{V_{id2}^5}{32(I_2/K)^2} + \dots \right). \quad (7)$$

The output current is expressed as the polynomial of the input signal with adjustable coefficients which are controlled by the voltages  $V_1$ ,  $V_2$ ,  $V_C$ . Finely adjusting the control voltage could suppress the intermodulation distortion of the analog predistortion system.

### 3. Circuit realization and measurement results

According to the circuit diagram of Fig. 3, an analog predistortion circuit was designed and realized in SMIC 0.18- $\mu\text{m}$  CMOS. The ratio of the transistor's gate channel width to the gate channel length ( $W/L$ ) for the source coupled transconductance differential amplifiers should be chosen to let the linear and nonlinear transfer characteristic be realizable. The SSGSS pad is used to minimize the area of the circuit. A photograph of the fabricated chip is shown in Fig. 4. The size of the chip is  $0.48 \times 0.24 \text{ mm}^2$ .

The analog predistortion circuit was measured with a directly modulated RF optical fiber link as shown in Fig. 5. An Agilent E4438C ESG VECTOR signal generator was used as the signal source, and an Agilent E4440A spectrum analyzer was used to measure the output spectrum. The semiconductor laser used was a 1310 nm InAlGaAs Fabry Perot laser in TO package and its threshold current was about 11 mA. A

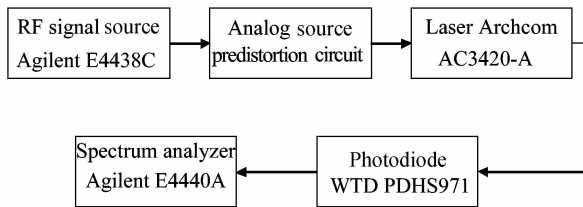
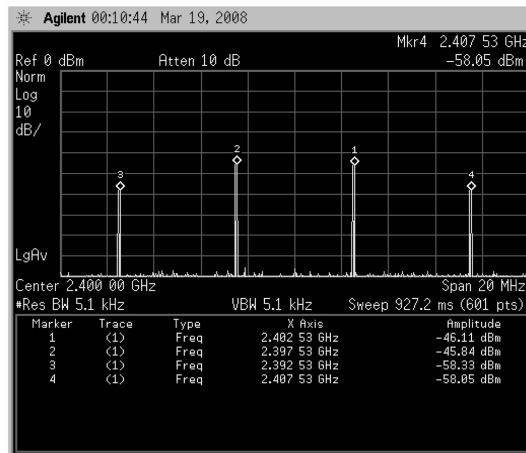
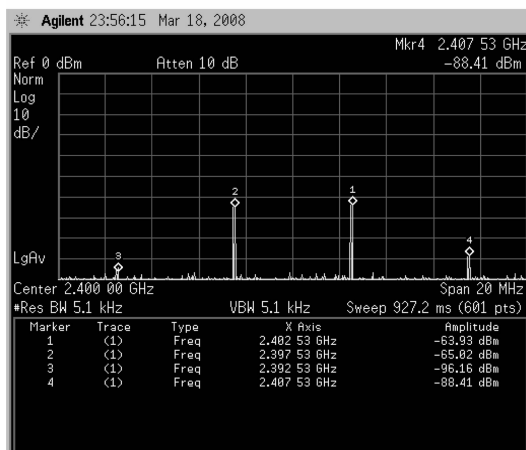


Fig. 5. IMD measurement setup.



(a)



(b)

Fig. 6. Two-tone IMP3 spectrum of the ROF link: (a) Without the predistortion circuit; (b) With the predistortion circuit.

GaInP/InP PIN detector with a 10 GHz bandwidth was used to detect the optical signal. By finely adjusting the control voltage and the bias voltage of the circuit, an improvement in the linearity of the RF optical fiber link could be observed.

Two-tone transmission experiments were performed with and without the analog predistortion circuit for the optical fiber link shown in Fig. 5. Figure 6 shows the output spectrum of the power of the fundamental frequency and the third-order intermodulation product (IMP3) for the optical fiber link. It can be seen from the figure that the linearity improvement of the optical fiber link is about 15 dB with the predistortion circuit.

Figure 7 shows the IMD suppression of the ROF link with and without the predistortion circuit under different input powers. Two closely spaced frequencies  $f_1$  and  $f_2$  were used to measure the IMP3 at  $2f_1 - f_2$  and  $2f_2 - f_1$ ; here,  $f_1$  is 2397.5 MHz and  $f_2$  is 2402.5 MHz. The IMD suppression here means

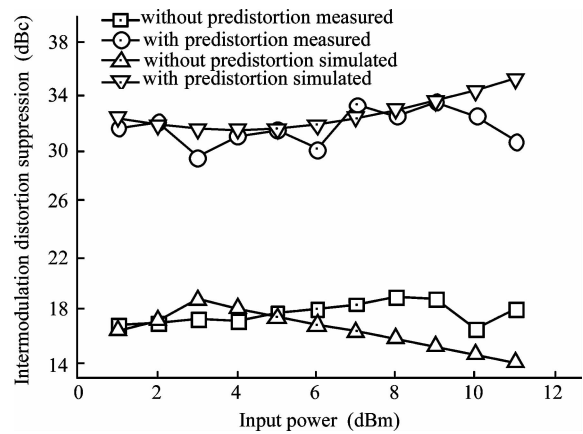


Fig. 7. Two-tone IMD suppression of the optical fiber link at  $f_1$  and  $2f_1 - f_2$  ( $f_1 = 2397.5$  MHz and  $f_2 = 2402.5$  MHz).

the difference of the output power between the fundamental signal at  $f_1$  and the IMP3 at  $2f_1 - f_2$ . The parameters of the semiconductor laser modules are characterized with the help of the Volterra model of semiconductor lasers and a circuit model based on the single-mode rate equations for semiconductor lasers is implemented<sup>[8]</sup>. The Spice model of the transistor provided by SMIC is converted and imported into the Advanced design system (ADS) software. A simulation of the nonlinear distortion of the semiconductor laser module and the predistortion system is realized in ADS with a harmonic balance simulator and the results are given in Fig. 7. It can be seen that at 2397.5 MHz the predistortion circuit can provide an improvement of 9 to 16 dBc to the IMD suppression of the optical fiber link.

#### 4. Conclusions

Approximating RF optical fiber links as a memoryless nonlinear system<sup>[9]</sup>, an analog predistortion circuit which predistorted the input signal to cancel or minimize the intermodulation distortion of the RF optical fiber link has been implemented in SMIC 0.18- $\mu$ m CMOS technology and tested with a directly modulated ROF link. Using the circuit, the third-order IMD suppression of the ROF link could be substantially improved by a value of 9 to 16 dBc at relatively low cost. The circuit could be integrated with a laser driver, or used to manually adjust the distortion of the ROF link in some applications.

#### References

- [1] Montebugnoli S, Boschi M, Perini F, et al. Large antenna array remoting using radio-over-fiber technologies for radio astronomical application. *Microw Opt Technol Lett*, 2005, 46(1): 48
- [2] Chung Y D, Choi K S, Sim J S, et al. A 60-GHz-band analog optical system-on-package transmitter for fiber-radio communications. *J Lightwave Technol*, 2007, 25(11): 3407
- [3] Ohmori S, Yamao V, Nakajima N. The future generation of mobile communications based on broadband access technologies. *IEEE Comm Mag*, 2000, 38(12): 134
- [4] Al-Raweshidy H, Komaki S. Radio over fiber technologies

- for mobile communication networks. Norwood: Artech House, 2002
- [5] Hassin D, Vahldieck R. Feedforward linearization of analog modulated laser diodes: theoretical analysis and experimental verification. *IEEE Trans Microw Theory Tech*, 1993, 41(12): 2376
- [6] Ghoniemy S. RF/fiber optical interface for microcellular wireless transceivers. Ottawa: Ottawa-Carleton Institute for Electrical and Computer Engineering, 2003
- [7] Lin F C, Holburn D M, Lalithambika V A, et al. Fully integrated CMOS VCSEL driver with nonlinearity suppression for RF optical fiber links. *Proceedings of SPIE*, 2004, 5356: 56
- [8] Salgado H M, O'Reilly J J. Experimental validation of Volterra series nonlinear modelling for microwave subcarrier optical systems. *IEE Proc Optoelectron*, 1996, 143(4): 209
- [9] Shah A R, Jalali B. Adaptive equalization for broadband pre-distortion linearization of optical transmitters. *IEE Proc Optoelectron*, 2005, 152(1): 16